Hindawi
International Journal of Aerospace Engineering
Volume 2020, Article ID 8853867, 8 pages
https://doi.org/10.1155/2020/8853867

Research Article

Treating the Solid Pendulum Motion by the Large Parameter Procedure

A. I. Ismail [1,2]

[1] *Mechanical Engineering Department, Faculty of Engineering and Islamic Architecture, Umm Al-Qura University, Makkah, Saudi Arabia P. O. Box 5555 Makkah*
[2] *Department of Mathematics, Faculty of Science, Tanta University, Tanta, P.O. Box 31527, Egypt*

Correspondence should be addressed to A. I. Ismail; aiismail@uqu.edu.sa

Received 5 September 2020; Revised 13 November 2020; Accepted 2 December 2020; Published 23 December 2020

Academic Editor: Jiaqiang E

In this paper, we consider the dynamical description of a pendulum model consists of a heavy solid connection to a nonelastic string which suspended on an elliptic path in a vertical plane. We suppose that the dimensions of the solid are large enough to the length of the suspended string, in contrast to previous works which considered that the dimensions of the body are sufficiently small to the length of the string. According to this new assumption, we define a large parameter ε and apply Lagrange's equation to construct the equations of motion for this case in terms of this large parameter. These equations give a quasi-linear system of second order with two degrees of freedom. The obtained system will be solved in terms of the generalized coordinates θ and φ using the large parameter procedure. This procedure has an advantage over the other methods because it solves the problem in a new domain when fails all other methods for solving the problem in such a domain under these conditions. It is one of the most important applications, when we study the slow spin motion of a rigid body in a Newtonian field of force under an external moment or the rotational motion of a heavy solid in a uniform gravity field or the gyroscopic motions with a sufficiently small angular velocity component about the major or the minor axis of the ellipsoid of inertia. There are many applications of this technique in aerospace science, satellites, navigations, antennas, and solar collectors. This technique is also useful in all perturbed problems in physics and mechanics, for example, the perturbed pendulum motions and the perturbed mechanical systems. The results of this paper also are useful in moving bridges and the swings. For satisfying the validation of the obtained solutions, we consider numerical considerations by one of the numerical methods and compare the obtained analytical and numerical solutions.

1. Introduction

The pendulum models have attracted scientists and researchers with many descriptions of motions and their analysis as important examples in physics and theoretical and applied dynamics. The most important pendulum motions come from the moving of a heavy particle suspended a light rod which is jointed pivotally at a point on the X-axis which rotates by an angular velocity ω about the horizontal fixed axis. In [1], the authors presented the elastic pendulum problem. They derived the equations of motion and gave real-life examples for elastic pendulum motions. Equilibrium states and trivial cases are studied. In [2], a harmonically excited spring pendulum motion with 3 degrees of freedom is considered. The authors were connected to a direct transversely tuned absorber. The authors used the multiple scale method for solving the system of equations of motion. They used the phase-plane method for applying the stability of the motion. They studied the influence of the tuned absorber and the parameters of the model on the change of the motion numerically. In [3], the elastic pendulum with resonance appearing at cubic approximation in the Lagrangian function was investigated. The modulated equations of motion were obtained. The authors used the Hamiltonian reduction technique to describe the dynamical behavior of this system. In [4], the approximated damping elastic pendulum model was considered. The authors derived the governing equation with six degrees of freedom. The natural frequencies are derived from the linearized system of equations. The stability diagrams are used to show regular periodicity. Due to damping, there are unstable waves (irregular) depending on the damping level and the amount of parametric excitation for the natural frequency. The article [5] presented the rotational motion in a plane for a mathematical pendulum when its axis swinging vertically and horizontally, so the axis path is an ellipse nears a circle. The study is considered as precise spin solutions for a circular axis path case with zero gravity. The existence of the stability conditions of these solutions is considered. Supposing that the excitation amplitude is not small and the coaxial path contains a small ellipsoid. Approximated solutions for both high and low linear damping are found. A comparison of approximate and digital solutions was performed for different values of the damping factor. In [6], the governing system of two generalized coordinates of a nonlinear dynamic model with the spring pendulum damped motion is considered in presence of the flow of an inviscid fluid. The motion control system is attained by applying the equations of Lagrange. The multiple scale procedure is used to solve the equations of motion for this system. The authors obtained approximated solutions of the 2^{nd} approximation. The resonance cases and the steady-state ones are studied. The stability procedure is given using the phase plane diagrams. In [7], the dynamics of nonlinear multiple degrees of freedom for a spring pendulum model moving in an auxiliary circle for the elliptical path are considered. Using the method of multiple scales, the authors solved the system of equations of motion. The temporal history of the solutions obtained and the phase plane projections are given to explain the dynamic behavior of the mentioned system.

In [8] the authors studied the elastic pendulum motion with resonance appearing at the third order in its Lagrange's approximation. The governing dynamical equations of motion and Hamiltonian reduction are obtained for this system. In [9], the frequencies of the elastic pendulum oscillations are in the ratio 2 : 1 which is named the pulsation. The dynamics of this problem and the modulation equations for the resonant motion with small amplitudes are obtained as 3 wave equations. The complete solutions are obtained by using the Hamiltonian reduction. The phases, amplitudes, and precession angles of the solutions are given. The validity of the obtained results is given in high accuracy by numerical experiments. The article [10] presented a dynamical behavior of an elastic pendulum model. The author assumed that the pendulum moves in a vertical plane which rotates with uniform angular velocity ω. The author used Lagrange's equations to find the differential equations of motion. The obtained equations are reduced to a nonlinear system of 2^{nd} order which is solved by the small parameter perturbed technique. Numerical considerations are obtained through the Matlab program. These considerations show the validity of both analytical and numerical solutions.

In [11], the nonlinear multiple degrees of freedom response is investigated for a normal dynamic system given by the spring pendulum moving in an elliptical path. The Lagrange equations were used to construct the governing system of equations for the motion. The multiple scale method is used for deriving the approximated solutions of the resonance system. The steady-state motions and the stabilities of the solutions are considered. The authors in [12] studied the problem of spring pendulum dynamics in the presence of pendulum absorber using the theory of nonlinear normal patterns and asymptotic numerical procedures. They investigated the dynamics of the pendulum for both low and high vibration amplitudes. Using different methods, the stability of the vibration patterns is analyzed. The authors in [13] studied the relative periodic solutions for an elastic pendulum motion of a rigid body with a corresponding suspended point moves on the auxiliary sphere of an ellipse. The Lagrange's function is applied to construct the equations of motion which are solved using the perturbed small parameter method. Numerical considerations are given using the Runge-Kutta method to prove the validity of the solutions.

In this article, we consider a heavy solid suspended in a string which suspended to an ellipse in a uniform vertical plane. The equations of motion for this mathematical pendulum in terms of the two degrees of freedom are obtained, and a large parameter depends on the model properties is assumed. By the definition of the large parameter, the approximated periodic solutions are obtained using the large parameter perturbed procedure. The accuracy of these solutions is investigated through a numerical technique and computerized programs.

2. Formulation of the Problem

Let us consider the coordinate system OXY on which X-axis is horizontal and Y-axis is downward vertical. A rigid body with mass m is suspended by a string of length ℓ which attached to a point O_1 moving on the ellipse. The point Q on the circle, which has the same center of the ellipse and its radius equals b such that the line AQ is normal to the largest axis of the ellipse, is called the corresponding point of the point O_1 on that circle. When the point O_1 moves on the ellipse, the point Q moves on the circle with a constant angular velocity ω (i.e., the angle between the line OQ and the Y -axis must depend on time t only). Let us assume that the angle between the straight line passing through O_2 and the center of gravity C of the body and the vertical will be denoted by φ, the angle of deflection of the string from the vertical straight line passing through O_1 will be denoted by θ, and the distance between the center of gravity of the body and the point O_2 will be denoted by h (i.e., $h = O_2C$) (see Figure 1). Choosing the body system of coordinates $C\xi\eta\zeta$ such that $C\eta$ passes through O_2, $C\xi$ is orthogonal to $C\eta$ and lying in the plane OXY, while $C\zeta$ is orthogonal to OXY.

We assume that the axes of the system $C\xi\eta\zeta$ represent the principal axes of inertia of the body. The principal moment of inertia concerning $C\xi$ will be denoted by J. The motion of the body starts at the instant $t = 0$ in the anticlockwise direction; after time t, the point O_1 is expected to make an angle $\theta = \omega t$ with the vertical axis.

The coordinate of the point C is (x_c, y_c) which takes the form

$$\begin{aligned} x_c &= a \sin \omega t + \ell \sin \theta + h \sin \varphi, \\ y_c &= b \cos \omega t + \ell \cos \theta + h \cos \varphi. \end{aligned} \tag{1}$$

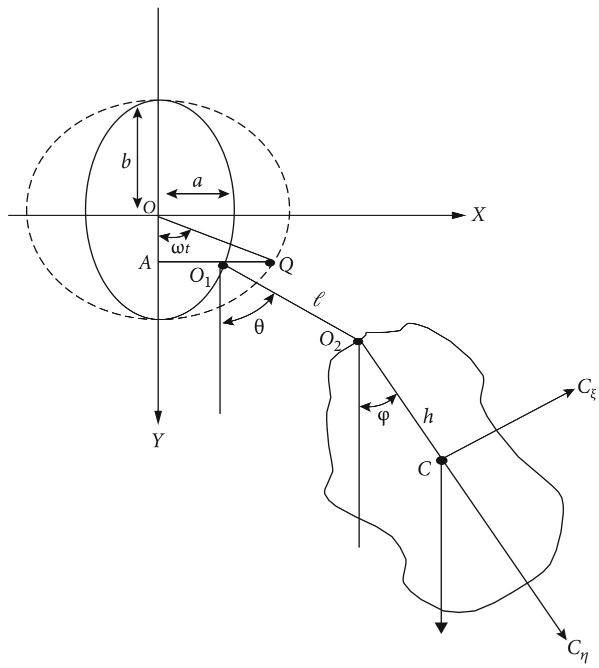

Figure 1: The pendulum model.

The kinetic energy of the system is

$$T = \frac{1}{2} m \left(\dot{x}_c^2 + \dot{y}_c^2\right) + \frac{1}{2} J \dot{\varphi}^2, \tag{2}$$

which takes the form

$$\begin{aligned} \mathbf{L} = \frac{1}{2} m \Big[& \ell^2 \dot{\theta}^2 + h^2 \dot{\varphi}^2 + \omega^2 \left(a^2 \cos^2 \omega t + b^2 \sin^2 \omega t\right) \\ & + 2\ell h \dot{\theta} \dot{\varphi} \cos(\theta - \varphi) + 2\ell \omega \dot{\theta} (a \cos \omega t \cos \theta \\ & + b \sin \omega t \sin \theta) + 2h\omega \dot{\varphi} (a \cos \varphi \cos \omega t \\ & + b \sin \varphi \sin \omega t) \Big] + \frac{1}{2} J \dot{\varphi}^2. \end{aligned} \tag{3}$$

The potential energy of the system can be expressed as follows:

$$\pi = -mg[\ell \cos \theta + h \cos \varphi]. \tag{4}$$

The Lagrangian of the system is [14]

$$L = T - \pi. \tag{5}$$

It can be written as follows:

$$\begin{aligned} \mathbf{L} = \frac{1}{2} m \Big[& \ell^2 \dot{\theta}^2 + h^2 \dot{\varphi}^2 + \omega^2 \left(a^2 \cos^2 \omega t + b^2 \sin^2 \omega t\right) \\ & + 2\ell h \dot{\theta} \dot{\varphi} \cos(\theta - \varphi) + 2\ell \omega \dot{\theta} (a \cos \omega t \cos \theta \\ & + b \sin \omega t \sin \theta) + 2h\omega \dot{\varphi} (a \cos \varphi \cos \omega t \\ & + b \sin \varphi \sin \omega t) \Big] + \frac{1}{2} J \dot{\varphi}^2 + mg(\ell \cos \theta + h \cos \varphi) \end{aligned} \tag{6}$$

Let us define the following parameters.

$$\begin{aligned} \varepsilon &= \frac{h}{\ell} \succ \succ 1, \\ \varepsilon \delta &= \frac{a}{\ell}, \\ \varepsilon \sigma &= \frac{b}{\ell}, \end{aligned} \tag{7}$$

where $\delta = a/h$, $\sigma = b/h$, and ε is a large parameter.

We introduce the variables

$$\Phi = \varepsilon^{-1} \varphi = \left(\frac{\ell}{h}\right) \varphi, \; \Theta = \varepsilon^{-1} \theta = \left(\frac{\ell}{h}\right) \theta, \; \tau = \omega t, \tag{8}$$

so that $d/dt = \omega(d/d\tau)$ and $d/d\tau = (')$.

The new Lagrangian function of the system can be written as follows:

$$\begin{aligned} \overset{*}{L} = \frac{1}{2} m \Big[& \omega^2 \ell^2 \varepsilon^{-2} \theta'^2 + \omega^2 h^2 \varepsilon^{-2} \varphi'^2 + \omega^2 \left(a^2 \cos^2 \tau + b^2 \sin^2 \tau\right) \\ & + 2\omega^2 \ell h \varepsilon^{-2} \theta' \varphi' \left(\cos \varepsilon^{-1} \theta \cos \varepsilon^{-1} \varphi + \sin \varepsilon^{-1} \theta \sin \varepsilon^{-1} \varphi\right) \\ & + 2\ell \varepsilon^{-1} \omega^2 \theta' \left(a \cos \tau \cos \varepsilon^{-1} \theta + b \sin \tau \sin \varepsilon^{-1} \theta\right) \\ & + 2h \varepsilon^{-1} \omega^2 \varphi' \left(a \cos \tau \cos \varepsilon^{-1} \varphi + b \sin \tau \sin \varepsilon^{-1} \varphi\right) \Big] \\ & + \frac{1}{2} J \varepsilon^{-2} \omega^2 \varphi'^2 + mg \left(\ell \cos \theta + h \cos \varepsilon^{-1} \varphi\right). \end{aligned} \tag{9}$$

For a small value of $\varepsilon^{-1}\theta, \varepsilon^{-1}\varphi$, we can expand the sines and cosines in the form of power series expansions to obtain

$$\begin{aligned} \overset{*}{L} = \frac{1}{2} m \omega^2 \Bigg\{ & \ell^2 \varepsilon^{-2} \theta'^2 + h^2 \varepsilon^{-2} \varphi'^2 + a^2 \cos^2 \tau + b^2 \sin^2 \tau \\ & + 2\ell h \varepsilon^{-2} \theta' \varphi' \left[\left(1 - \frac{\varepsilon^{-2} \theta^2}{2}\right) \left(1 - \frac{\varepsilon^{-2} \varphi^2}{2}\right) \right. \\ & \left. + \left(\varepsilon^{-1} \theta - \frac{\varepsilon^{-3} \theta^3}{6}\right) \left(\varepsilon^{-1} \varphi - \frac{\varepsilon^{-3} \varphi^3}{6}\right) \right] + 2\ell \varepsilon^{-1} \theta' \\ & \cdot \left[a \cos \tau \left(1 - \frac{\varepsilon^{-2} \theta^2}{2}\right) + b \sin \tau \left(\varepsilon^{-1} \theta - \frac{\varepsilon^{-3} \theta^3}{6}\right) \right] \\ & + 2h \varepsilon^{-1} \varphi' \left[a \cos \tau \left(1 - \frac{\varepsilon^{-2} \varphi^2}{2}\right) \right. \\ & \left. + b \sin \tau \left(\varepsilon^{-1} \varphi - \frac{\varepsilon^{-3} \varphi^3}{6}\right) \right] \Bigg\} + \frac{1}{2} J \varepsilon^{-2} \omega^2 \varphi'^2 \\ & + mg \left[\ell \left(1 - \frac{\varepsilon^{-2} \theta^2}{2}\right) + h \left(1 - \frac{\varepsilon^{-2} \varphi^2}{2}\right) \right]. \end{aligned} \tag{10}$$

3. Equations of Motion

According to Lagrange's equations [15],

$$\frac{d}{d\tau}\left(\frac{\partial L^*}{\partial q_i'}\right) - \frac{\partial L^*}{\partial q_i} = 0, \quad (i = 1, 2), \tag{11}$$

where q_i are the generalized coordinates and $q_i{}'$ are the generalized velocities, and we take the coordinates $q_1 = \theta$ and $q_2 = \varphi$.

Introducing the parameters

$$\begin{aligned} \omega_n^2 &= \frac{g}{\ell\omega^2}, \\ \gamma &= \frac{\ell^2}{h^2 + (J/m)}, \\ \Omega^2 &= \frac{gh}{h^2 + (J/m)}, \end{aligned} \tag{12}$$

where g is the acceleration of gravity; the system of differential equations of motion can be written as follows:

$$\begin{aligned} \theta'' + \omega_n^2\theta &= \delta \sin\tau - \varepsilon^{-1}\left(\theta'' + \theta\sigma\cos\tau\right) \\ &\quad - \frac{1}{2}\varepsilon^{-2}\theta^2\delta\sin\tau + \varepsilon^{-3}\left(\frac{1}{2}\varphi''\theta^2 + \frac{\varphi''}{2}\varphi^2\right. \\ &\quad \left. - \theta\varphi\varphi'' - \varphi'^2\theta + \varphi'^2\varphi + \frac{\theta^3}{6}\sigma\cos\tau\right), \end{aligned} \tag{13}$$

$$\begin{aligned} \varphi'' + \Omega^2\varphi &= \varepsilon^{-1}\gamma\left(-\theta'' + \delta\sin\tau\right) + \varepsilon^{-3}\gamma\left(\frac{1}{2}\theta''\theta^2\right. \\ &\quad + \frac{1}{2}\theta''\varphi^2 - \theta''\theta\varphi + \theta'^2\theta - \theta'^2\varphi \\ &\quad \left. - \frac{\delta}{2}\varphi^2\sin\tau - \sigma\varphi\cos\tau\right). \end{aligned} \tag{14}$$

The expressions Θ and Φ are expected to be functions of a large parameter ε and dependent on the values of γ, ω_n, and Ω.

4. Approximate Periodic Solutions

Now, to find the perturbed solution of the nonresonance case up to the second approximation, we apply the method of the large parameter [16] in the following form.

$$\begin{aligned} \Theta(\tau,\varepsilon) &= \theta_0(\tau) + \varepsilon^{-1}\theta_1(\tau) + \varepsilon^{-2}\theta_2(\tau) + \cdots, \\ \Phi(\tau,\varepsilon) &= \varphi_0(\tau) + \varepsilon^{-1}\varphi_1(\tau) + \varepsilon^{-2}\varphi_2(\tau) + \cdots. \end{aligned} \tag{15}$$

Substituting from (15) into (13) and (14) and equating to zero each coefficient of $(1/\varepsilon)$, we find that

Coefficient of $(1/\varepsilon)^0$

$$\begin{aligned} \theta_0'' + \omega_n^2\theta_0 &= \delta\sin\tau, \\ \varphi_0'' + \Omega^2\varphi_0 &= 0. \end{aligned} \tag{16}$$

Coefficient of $(1/\varepsilon)$

$$\begin{aligned} \theta_1'' + \omega_n^2\theta_1 &= -\varphi_0'' - \theta_0\sigma\cos\tau, \\ \varphi_1'' + \Omega^2\varphi_1 &= \gamma\left(\delta\sin\tau - \theta_0''\right). \end{aligned} \tag{17}$$

Coefficient of $(1/\varepsilon)^2$

$$\begin{aligned} \theta_2'' + \omega_n^2\theta_2 &= -\varphi_1'' - \theta_1\sigma\cos\tau - \frac{1}{2}\delta\theta_0^2\sin\tau, \\ \varphi_2'' + \Omega^2\varphi_2 &= -\gamma\theta_1''. \end{aligned} \tag{18}$$

Coefficient of $(1/\varepsilon)^3$

$$\begin{aligned} \theta_3'' + \omega_n^2\theta_3 &= -\varphi_2'' - \theta_2\sigma\cos\tau + \delta\theta_0^2\theta_1\sin\tau \\ &\quad - \frac{1}{2}\varphi_0''\theta_0^2 - \frac{1}{2}\varphi_0''\varphi_0^2 + \theta_0\varphi_0\varphi_0'' \\ &\quad + \varphi'^2_0\theta_0 - \varphi'^2_0\varphi_0 - \frac{\theta_0^3}{6}\sigma\cos\tau, \end{aligned} \tag{19}$$

$$\begin{aligned} \varphi_3'' + \Omega^2\varphi_3 &= \gamma\left(-\theta_2'' + \frac{1}{2}\theta_0''\theta_0^2 + \frac{1}{2}\theta_0''\varphi_0^2 - \theta_0''\theta_0\varphi_0 + \theta'^2_0\theta_0\right. \\ &\quad \left. - \theta'^2_0\varphi_0 - \frac{\delta}{2}\varphi_0^2\sin\tau - \sigma\varphi_0\cos\tau\right). \end{aligned} \tag{20}$$

Making use of the equations (15)-(20), the required periodic solutions take the form

$$\begin{aligned} \Theta(\tau,\varepsilon) &= \frac{\delta}{(\omega_n^2 - 1)}\sin\tau + \varepsilon^{-1}\left[\frac{\Omega^2 A}{(\omega_n^2 - \Omega^2)}\cos\Omega\tau\right. \\ &\quad \left. + \frac{\Omega^2 B}{(\omega_n^2 - \Omega^2)}\sin\Omega\tau - \frac{\sigma\delta}{2(\omega_n^2 - 1)(\omega_n^2 - 4)}\sin 2\tau\right] \\ &\quad + \varepsilon^{-2}\left[\frac{\gamma\delta\omega_n^2}{(\omega_n^2 - 1)^2(\Omega^2 - 1)}\sin\tau\right. \\ &\quad - \frac{\Omega^2\sigma A}{2(\omega_n^2 - \Omega^2)(\omega_n^2 - (1+\Omega)^2)}\cos(1+\Omega)\tau \\ &\quad - \frac{\Omega^2\sigma A\cos(\Omega - 1)\tau}{2(\omega_n^2 - \Omega^2)(\omega_n^2 - (\Omega - 1)^2)} \\ &\quad - \frac{\Omega^2 B\sigma\sin(\Omega + 1)\tau}{2(\omega_n^2 - \Omega^2)(\omega_n^2 - (\Omega + 1)^2)} \end{aligned}$$

$$- \frac{\Omega^2 B\sigma \sin(\Omega - 1)\tau}{2(\omega_n^2 - \Omega^2)(\omega_n^2 - (\Omega - 1)^2)} + \frac{\sigma^2 \delta \cos\tau}{4(\omega_n^2 - 1)^2(\omega_n^2 - 4)} - \frac{\sigma^2\delta\cos 3\tau}{4(\omega_n^2 - 1)(\omega_n^2 - 4)(\omega_n^2 - 9)} - \frac{3\delta^3 \sin\tau}{8(\omega_n^2 - 1)^3} + \frac{\delta^3 \sin 3\tau}{8(\omega_n^2 - 1)(\omega_n^2 - 9)}\Bigg], \tag{21}$$

$$\Phi(\tau, \varepsilon) = A\cos\Omega\tau + B\sin\Omega\tau + \varepsilon^{-1}\frac{\gamma\delta\omega_n^2}{(\Omega^2 - 1)(\omega_n^2 - 1)}\sin\tau - \varepsilon^{-2}\frac{2\gamma\sigma\delta\sin 2\tau}{(\omega_n^2 - 1)(\omega_n^2 - 4)(\Omega^2 - 4)}. \tag{22}$$

Neglecting the secular terms [17] in the formulas (21) and (22), the constants A and B will vanish; then,

$$\Theta(\tau, \varepsilon) = \frac{\delta}{\omega_n^2 - 1}\sin\tau - \frac{\varepsilon^{-1}\sigma\delta\sin 2\tau}{2(\omega_n^2 - 1)(\omega_n^2 - 4)} + \varepsilon^{-2}\Bigg[\frac{\gamma\,\delta\,\omega_n^2}{(\omega_n^2 - 1)^2(\Omega^2 - 1)}\sin\tau + \frac{\sigma^2\delta\cos\tau}{4(\omega_n^2 - 1)^2(\omega_n^2 - 4)} - \frac{\sigma^2\delta\cos 3\tau}{4(\omega_n^2 - 1)^2(\omega_n^2 - 4)(\omega_n^2 - 9)} - \frac{3\delta^3}{8(\omega_n^2 - 1)^3}\sin\tau + \frac{\delta^3}{8(\omega_n^2 - 1)^2(\omega_n^2 - 9)}\sin 3\tau\Bigg] + \cdots,$$

$$\Phi(\tau, \varepsilon) = \varepsilon^{-1}\frac{\gamma\delta\omega_n^2\sin\tau}{(\omega_n^2 - 1)(\Omega^2 - 1)} - \varepsilon^{-2}\frac{2\gamma\sigma\delta\sin 2\tau}{(\omega_n^2 - 1)(\omega_n^2 - 4)(\Omega^2 - 4)} + \cdots. \tag{23}$$

5. Discussion of the Results

In this subsection, we give a parametric analysis of the obtained results for the behavior of the obtained analytical solutions Θ and Φ as functions dependent on the time τ, the valuesγ, ω_n, Ω, δ, and σ, and the large parameter ε; that is,

$$\Theta = \Theta(\tau, \gamma, \omega_n, \Omega, \delta, \sigma, \varepsilon),$$
$$\Phi = \Phi(\tau, \gamma, \omega_n, \Omega, \delta, \sigma, \varepsilon). \tag{24}$$

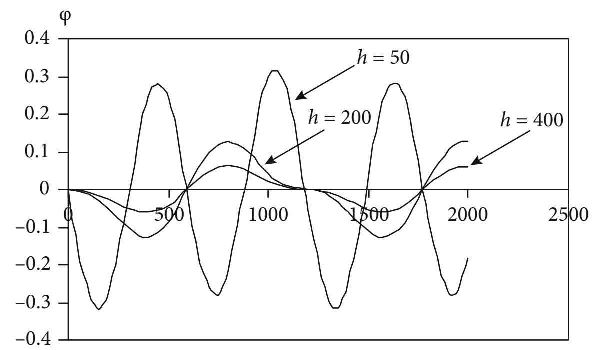

Figure 2: The analytical and numerical solutions φ against τ at h = 400, 200, and 50.

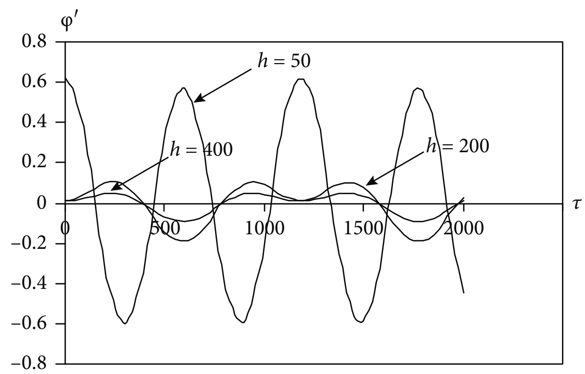

Figure 3: The analytical and numerical angular velocities φ' against τ at $h = 400$, 200, and 50.

We note that the domain of the obtained solutions under the assumed conditions is as follows:

$$\Theta = \Theta(\tau, \gamma \longrightarrow 0, \omega_n \longrightarrow \infty, \Omega \longrightarrow 0, \delta \longrightarrow 0, \sigma \longrightarrow 0, \varepsilon \longrightarrow \infty),$$
$$\Phi = \Phi(\tau, \gamma \longrightarrow 0, \omega_n \longrightarrow \infty, \Omega \longrightarrow 0, \delta \longrightarrow 0, \sigma \longrightarrow 0, \varepsilon \longrightarrow \infty), \tag{25}$$

while the domain of the previous corresponding cases is as follows:

$$\Theta = \Theta(\tau, \gamma \longrightarrow \infty, \omega_n \longrightarrow 0, \Omega \longrightarrow \infty, \delta \longrightarrow \infty, \sigma \longrightarrow \infty, \varepsilon \longrightarrow 0),$$
$$\Phi = \Phi(\tau, \gamma \longrightarrow \infty, \omega_n \longrightarrow 0, \Omega \longrightarrow \infty, \delta \longrightarrow \infty, \sigma \longrightarrow \infty, \varepsilon \longrightarrow 0). \tag{26}$$

This means that the obtained solutions are treated in a new domain which is considered as a complement space for the previous work domains.

In what follow, we study the validity of both analytical and numerical solutions. Using one of the numerical methods, we obtain numerical solutions and give more analysis of the results. The graphical representations for both solutions are obtained through computer programming.

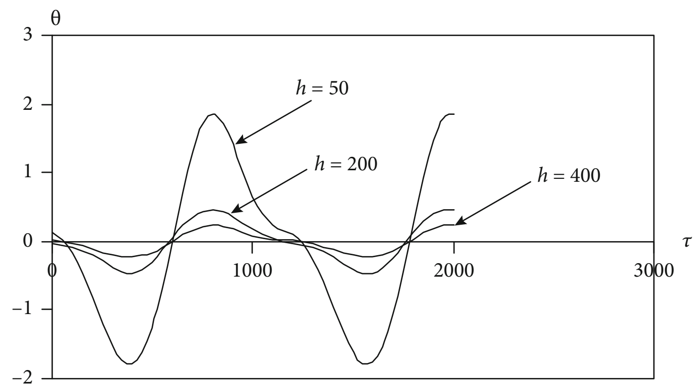

Figure 4: The analytical and numerical solutions θ against τ at $h = 400$, 200, and 50.

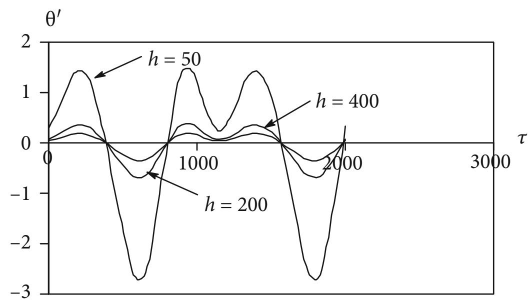

Figure 5: The analytical and numerical angular velocities θ' against τ at $h = 400$, 200, and 50.

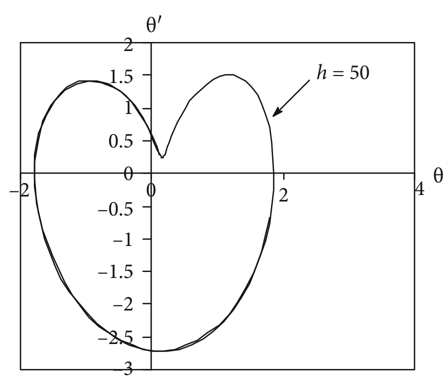

Figure 6: The analytical and numerical stabilities θ' against θ at $h = 50$.

6. Computerized Data

This section is devoted to ascertaining the accuracy of the solutions being considered in Sections 3 and 4. Computer programs are developed for the representation of the obtained analytical solutions θ and φ and their derivatives in a definite period. On the other hand, the fourth-order Runge-Kutta method [18] is applied to solve the autonomous system (13) and (14) for obtaining the numerical solutions and their derivatives and investigating their graphical representations. The characteristic curves for both the analytical and numerical solutions and their derivatives appear in Figures 2–5. From Figures 2 and 3, we deduce that when h increases, the number of the waves and their amplitudes of the solutions φ and φ' decrease and vice versa, while from Figures 4 and 5, we deduce that when h increases, the number of the waves is the same as the solutions θ and θ' but their amplitudes decrease and vice versa. The phasing diagram procedures [19] for the stability of the solutions are given in Figures 6–11. From these figures, we deduce that the solutions and their derivatives are stable but their amplitudes

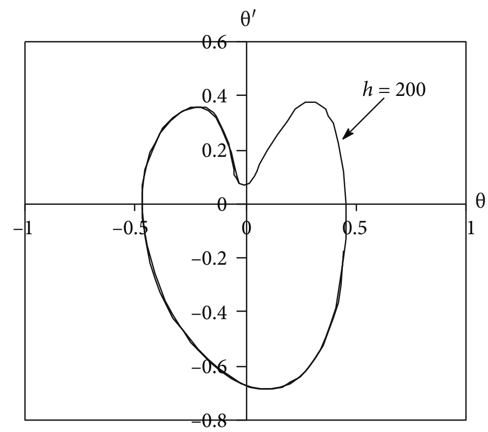

Figure 7: The analytical and numerical stabilities θ' against θ at $h = 200$.

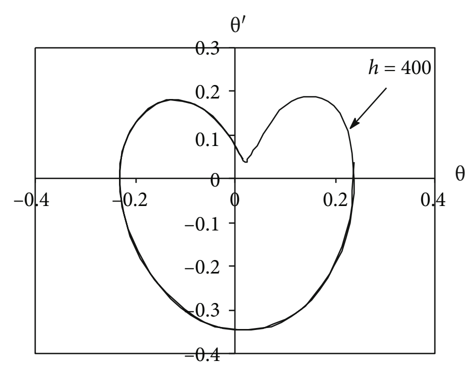

Figure 8: The analytical and numerical stabilities θ' against θ at $h = 400$.

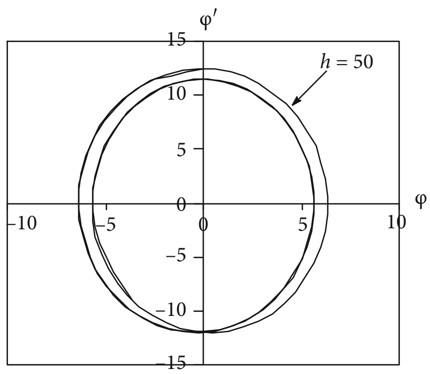

Figure 9: The analytical and numerical stabilities φ' against φ at $h = 50$.

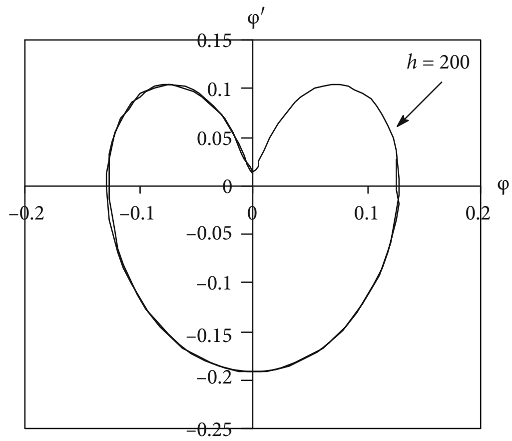

Figure 10: The analytical and numerical stabilities φ' against φ at $h = 200$.

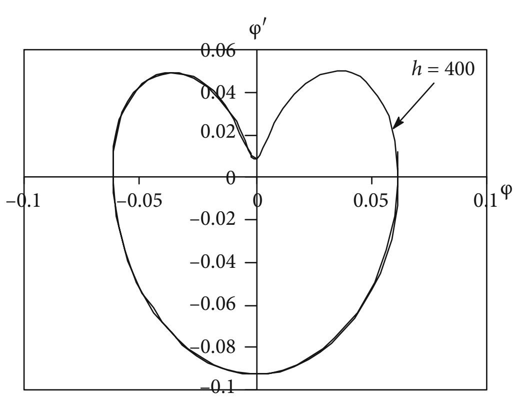

Figure 11: The analytical and numerical stabilities φ' against φ at $h = 400$.

decrease with increasing h. In all stability figures, the curves take the cardioid form except Figure 9. We deduce from Figures 2–5 that the analytical and numerical solutions are in full agreement, and Figures 6–11 show that the stability diagrams are largely identical. That is, the numerical results are largely correspondence with the analytical ones which prove the validation of both solutions and the used techniques.

7. Conclusion

This motion is very important as a mathematical pendulum model for many problems in fluid materials and gas translation in big and small tanks and is considered as a generalization for the problem studied in [11]. The description of the motion of this pendulum model is given. The equations of motion are obtained in terms of two degrees of freedom. New conditions for the motion are considered when the length of the string and radii of the ellipse are sufficiently small comparing to the dimensions of the solid body. A large parameter ε is constructed such that $\varepsilon = h/\ell$. Using the large parameter technique, we solve this problem in terms of two degrees of freedom θ and φ. The large parameter procedure gives us the chance to study the motion in new conditions and a new domain of the solutions. The obtained analytical solutions are represented graphically through a computer program. On the other hand, the fourth-order Runge-Kutta numerical technique is used to show the validity of the solutions. The obtained phasing diagrams prove full agreement of the obtained analytical and numerical solutions. We deduce also that the change of the parameters of the solid body affects the behavior of the obtained solutions. For example, the increase in h for the solutions of φ and φ' gives a decrease in the number and amplitude of the waves and vice versa, while the increase of h for the solutions θ and θ' gives a decrease in the amplitudes of these solutions with the same number of the waves. When $h \to \infty$, we have a straightened wave of the motion and the number of the waves is infinite.

Data Availability

Data sharing is not applicable to this article as no datasets were generated or analyzed during the current study.

Conflicts of Interest

The author declares that he has no competing interests.

References

[1] L. N. Hand and J. D. Finch, *Analytical Mechanics*, Cambridge University Press, 2008.

[2] M. Eissa and M. Sayed, "Vibration reduction of a three DOF non-linear spring pendulum," *Communications in Nonlinear Science and Numerical Simulation*, vol. 13, no. 2, pp. 465–488, 2008.

[3] D. D. Holm and P. Lynch, "Stepwise precession of the resonant swinging spring," *SIAM Journal on Applied Dynamical Systems*, vol. 1, no. 1, pp. 44–64, 2002.

[4] J. Orszaghova, H. Wolgamot, S. Draper, R. Eatock Taylor, P. H. Taylor, and A. Rafiee, "Transverse motion instability of a submerged moored buoy," *Proceedings of the Royal Society A: Mathematical, Physical and Engineering Sciences*, vol. 475, no. 2221, article 20180459, 2019.

[5] O. Anton, “On rotational solutions for elliptically excited pendulum,” *Physics Letters A*, vol. 375, no. 25, pp. 2524–2530, 2011.

[6] M. A. Bek, T. S. Amer, M. A. Sirwah, J. Awrejcewicz, and A. A. Arab, “The vibrational motion of a spring pendulum in a fluid flow,” *Results in Physics*, vol. 19, p. 103465, 2020.

[7] T. S. Amer, M. A. Bek, and M. K. Abouhmr, “On the vibrational analysis for the motion of a harmonically damped rigid body pendulum,” *Nonlinear Dynamics*, vol. 91, no. 4, pp. 2485–2502, 2018.

[8] J. Walker, *Principles of Physics*, Wiley, Hoboken, N.J., 9th edition, 2011.

[9] P. Lynch and C. Houghton, “Pulsation and precession of the resonant swinging spring,” *Physica D: Nonlinear Phenomena*, vol. 190, no. 1-2, pp. 38–62, 2004.

[10] T. S. Amer, “The dynamical behavior of a rigid body relative equilibrium position,” *Advances in Mathematical Physics*, vol. 2017, Article ID 8070525, 13 pages, 2017.

[11] T. S. Amer, M. A. Bek, and I. S. Hamada, “On the motion of harmonically excited spring pendulum in elliptic path near resonances,” *Advances in Mathematical Physics*, vol. 2016, Article ID 8734360, 15 pages, 2016.

[12] A. A. Klimenko, Y. V. Mikhlin, and J. Awrejcewicz, “Nonlinear normal modes in pendulum systems,” *Nonlinear Dynamics*, vol. 70, no. 1, pp. 797–813, 2012.

[13] A. I. Ismail, “Relative periodic motion of a rigid body pendulum on an ellipse,” *Journal of Aerospace Engineering*, vol. 22, no. 1, pp. 67–77, 2009.

[14] R. Starosta, G. Sypniewska-Kaminska, and J. Awrejcewicz, “Asymptotic analysis of kinematically excited dynamical systems near resonances,” *Nonlinear Dynamics*, vol. 68, no. 4, pp. 459–469, 2012.

[15] M. Eissa, M. Kamel, and A. T. El-Sayed, “Vibration reduction of multi-parametric excited spring pendulum via a transversally tuned absorber,” *Nonlinear Dynamics*, vol. 61, no. 1-2, pp. 109–121, 2010.

[16] A. I. Ismail, “Solving a problem of rotary motion for a heavy solid using the large parameter method,” *Advances in Astronomy*, vol. 2020, Article ID 2764867, 7 pages, 2020.

[17] T. S. Amer and M. A. Bek, “Chaotic responses of a harmonically excited spring pendulum moving in circular path,” *Nonlinear Analysis. Real-World Applications*, vol. 10, no. 5, pp. 3196–3202, 2009.

[18] V. Ruas, *Numerical Methods for Partial Differential Equations: An Introduction*, Jhon Wiley & Sons Ltd, 2016.

[19] http://ddebiftool.sourceforge.net/demos/neuron/html/demo1_psol.html.